Endlessly single-mode photonic crystal fiber

T. A. Birks, J. C. Knight, and P. St. J. Russell

Optoelectronics Group, School of Physics, University of Bath, Claverton Down, Bath, BA2 7AY, UK

Received March 10, 1997

We made an all-silica optical fiber by embedding a central core in a two-dimensional photonic crystal with a micrometer-spaced hexagonal array of air holes. An effective-index model confirms that such a fiber can be single mode for any wavelength. Its useful single-mode range within the transparency window of silica, although wide, is ultimately bounded by a bend-loss edge at short wavelengths as well as at long wavelengths.

In a previous Letter[1] we reported the fabrication of a photonic crystal fiber. This optical fiber was made entirely from undoped fused silica. The cladding was a two-dimensional photonic crystal made of silica with air holes running along the length of the fiber. The holes were arranged in a hexagonal honeycomb pattern across the cross section. The central hole was absent, leaving a silica defect that acted as the core (Fig. 1). The fiber was single mode over a remarkably wide wavelength range, from 458 to 1550 nm at least. Subsequent measurements have extended this range to 337 nm.

In a standard step-index fiber with core radius ρ and core and cladding indices n_{co} and n_{cl}, the number of guided modes is determined by the V value[2]:

$$V = (2\pi\rho/\lambda)({n_{\mathrm{co}}}^2 - {n_{\mathrm{cl}}}^2)^{1/2}\,, \tag{1}$$

which must be less than 2.405 for the fiber to be single mode. Thus single-mode fibers are in fact multimode for light of sufficiently short wavelength. We explained the wide single-mode range of the photonic crystal fiber by considering the effective refractive index of the cladding, loosely understood as the average index in the cladding weighted by the intensity distribution of the light. At shorter wavelengths the field becomes more concentrated in the silica regions and avoids the holes (as we observed by examination of the near-field patterns[1]), thus raising the effective cladding index. This dispersion counteracts the explicit dependence of V on wavelength λ and so extends the single-mode range. We now quantify this model and demonstrate that photonic crystal fibers can be single mode for all wavelengths. The model's validity is confirmed by bend-loss measurements, which show that the useful spectral range of the fiber is bounded by bend-loss edges at both short and long wavelengths.

Although most interest in photonic crystals has focused on their photonic bandgap properties, we do not consider guidance by photonic bandgap effects[3] here. Instead, because the core index is greater than the average index of the cladding, the fiber can guide by total internal reflection as a standard fiber does, despite the unconventional structure. That is, there are propagation constants β available to light in the core but not to light propagating in the cladding:

$$kn_0 > \beta > \beta_{\mathrm{FSM}}\,, \tag{2}$$

where $k = 2\pi/\lambda$, n_0 is the index of silica (the core material), and β_{FSM} is the propagation constant of the fundamental space-filling mode (FSM). The FSM is the fundamental mode of the infinite photonic crystal cladding if the core is absent, so β_{FSM} is the maximum β allowed in the cladding. Inasmuch as the lower limit of β in a step-index fiber is kn_{cl}, we identify the effective cladding index n_{eff} with

$$n_{\mathrm{eff}} = \beta_{\mathrm{FSM}}/k\,. \tag{3}$$

The FSM is the generalization of a z-directed plane wave in an infinite uniform medium, whose β equals $k \times$ the medium's index. Thus Eq. (3) gives the correct value in this special case. More generally, Eq. (3) is justified because inequality (2) implies that the transverse wave-vector component k_T in the core lies between zero and $k_{T\max} = (k^2{n_0}^2 - {\beta_{\mathrm{FSM}}}^2)^{1/2}$ for a guided mode. k_T is quantized by the boundary conditions between core and cladding, so the number of guided modes is determined by $\rho k_{T\max}$. For a step-index fiber this is simply the V value of Eq. (1). Thus

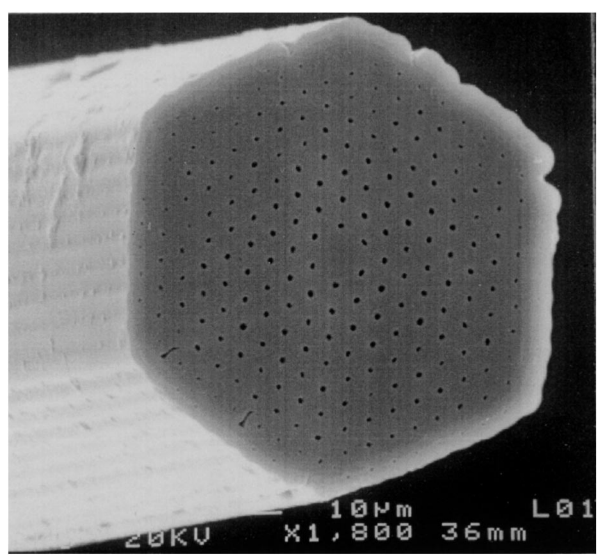

Fig. 1. Scanning electron microscope image of the end of a photonic crystal fiber, showing the central core where a hole has been omitted. The pitch Λ is 2.3 μm, and the fiber is ~40 μm across.

0146-9592/97/130961-03$10.00/0

β_{FSM}/k plays the role of an effective cladding index when one is counting modes, and so an effective V value such as Eq. (1) can be defined for the photonic crystal fiber:

$$V_{\mathrm{eff}} = (2\pi\Lambda/\lambda)(n_0{}^2 - n_{\mathrm{eff}}{}^2)^{1/2}, \tag{4}$$

which determines whether the fiber is single mode. As usual, when defining V values[2] one may choose any transverse dimension for ρ. Here we use the pitch (center–center spacing) of the holes Λ, which is also roughly the radius of the defect core formed by omitting one of them.

Having found n_{eff}, we consider the limit $\lambda \to 0$. The scalar wave equation, valid here,[4] gives

$$\Lambda^2\nabla_t{}^2\psi + V_{\mathrm{eff}}{}^2\psi = 0 \tag{5}$$

for the field distribution ψ of the FSM in silica regions, where $\nabla_t{}^2$ is the transverse part of the Laplacian operator. When $\lambda \to 0$, ψ is excluded from the low-index air holes[4] and is confined to the silica region bounded by the edges of the holes. For a given ratio of hole size to Λ, ψ is therefore an invariant function of normalized transverse coordinates x/Λ and y/Λ in the short-wavelength limit. Equation (5) then implies that V_{eff} is finite and independent of λ and Λ under these conditions. This situation contrasts with that for the step-index fiber, for which $V \to \infty$ as $\lambda \to 0$. The limiting value of V_{eff} depends on the relative size of the holes, but a sufficiently small value guarantees single-mode operation for all wavelengths λ and scales Λ.

By averaging the square of the refractive index in the photonic crystal cladding it is simple to show that the long-wavelength limit of V_{eff} in a scalar approximation is

$$V_{\mathrm{eff}} = k\Lambda F^{1/2}(n_0{}^2 - n_a{}^2)^{1/2}, \tag{6}$$

where n_a is the index of air (or whatever is in the holes) and F is the air filling fraction.

V_{eff} can be calculated in the general case in a scalar approximation. Because the FSM is a fundamental mode with the same symmetries as the photonic crystal itself, one finds it by solving the scalar wave equation within a unit cell centered on one of the holes of diameter d (Fig. 2). By reflection symmetry, the boundary condition at the edge is that $\partial\psi/\partial s = 0$, where s is a coordinate normal to the edge. We approximate this with a circular outer boundary at radius $r = b$, where $d\psi/dr = 0$. This is reasonable if the holes are not too large, because the field variation on a circle intersecting the hexagonal boundary will be small. Equating the model's filling fraction to the actual value gives b. The analysis is little more complicated than that of the step-index fiber[2]: The field in both regions is expressed in terms of Bessel functions of order 0, and the application of boundary conditions yields β_{FSM}. The resulting curves of V_{eff} against Λ/λ for $n_0 = 1.45$ and $n_a = 1.00$ are shown in Fig. 3 for various relative hole sizes d/Λ. The $\lambda \to 0$ limit of V_{eff} approaches zero slowly as d/Λ approaches zero.

The fiber described in our earlier Letter[1] has $\Lambda = 2.3\ \mu\mathrm{m}$ and $d/\Lambda \approx 0.15$, and the available wavelength range corresponds to Λ/λ between 1.5 and 6.8. V_{eff} is therefore less than 2.405 at all wavelengths. Although single-mode operation will not be defined by $V_{\mathrm{eff}} < 2.405$ specifically (perhaps our fiber becomes multimode at shorter wavelengths), some similar cutoff value V_{co} should apply. It is always possible to adjust d/Λ so that $V_{\mathrm{eff}} < V_{\mathrm{co}}$, thus proving that the photonic crystal fiber can indeed be endlessly single mode.

Larger holes make the fiber likely to be multimoded. The gaps between the holes become narrower, isolating the core more strongly from the silica in the cladding. Smaller holes make single-mode guidance more likely, but the decrease in effective index difference (or in effective N.A.) makes the fiber more susceptible to bend loss. A well-known simple expression gives the critical bend radius R_c at which bend loss in a waveguide becomes large.[5] Although it is not quantitatively accurate, it does give the correct parametric dependence of R_c on wavelength, core size, and refractive indices. The condition on bend radius R for low loss can be written as

$$R \gg R_c = \frac{8\pi^2 n_{\mathrm{co}}{}^2\rho^3}{\lambda^2 W^3}, \tag{7}$$

where W is the dimensionless modal parameter of optical fiber theory[2] and is a function of V only. For long wavelengths, the photonic crystal fiber behaves as a standard fiber, as anticipated in Eq. (6). W^3 decreases more rapidly[2] than λ^{-2} with increasing λ,[2] so there is a long-wavelength bend-loss edge beyond which the fiber suffers massive bend loss.

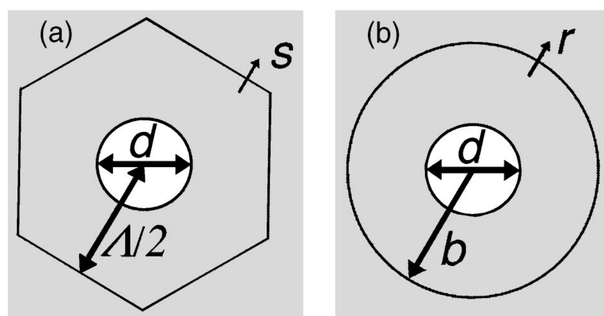

Fig. 2. (a) Actual unit cell in the photonic crystal with (b) its circular approximation.

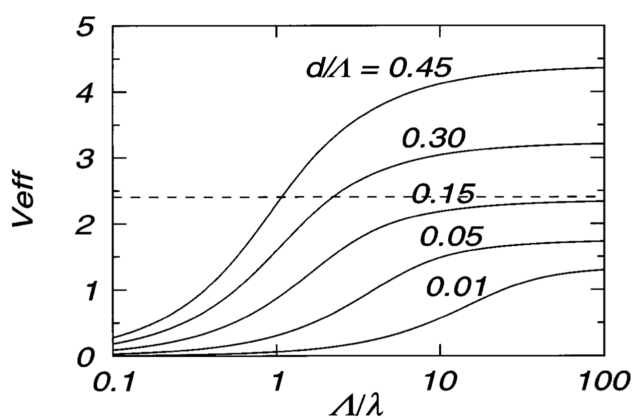

Fig. 3. Variation of V_{eff} with Λ/λ for various relative hole diameters d/Λ. The dashed line marks $V_{\mathrm{eff}} = 2.405$, the cutoff V value for a step-index fiber.

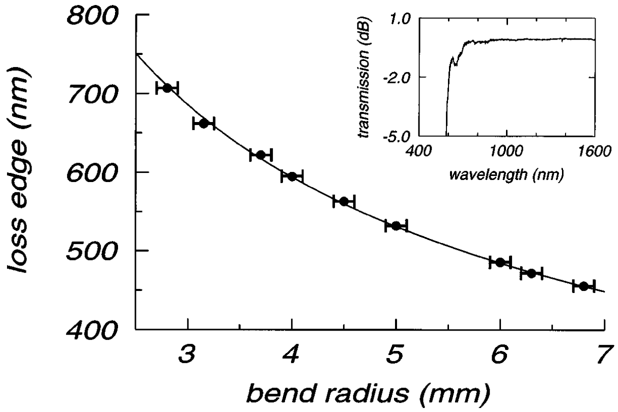

Fig. 4. Measured short-wavelength loss edge (for 3-dB loss) versus bend radius for a photonic crystal fiber with a single-turn bend (points), together with a fit to $\lambda = \text{constant}/\sqrt{R}$. Inset: Typical transmission spectrum of the bent fiber, relative to the transmission of the straight fiber. The short-wavelength loss edge lies near 600 nm. The long-wavelength loss edge is beyond the range of the measurement for this sample.

For short wavelengths the fibers are quite different. In standard fiber,[2] $W \propto \rho/\lambda$, giving $R_c \sim \lambda$ independently of the core diameter. However, V_{eff} and hence W are constant in the photonic crystal fiber, so R_c varies as

$$R_c \propto \Lambda^3/\lambda^2\,. \tag{8}$$

The reciprocal dependence on λ implies that there is a short-wavelength bend-loss edge also. Measurements of the transmission spectrum of a photonic crystal fiber were taken for a range of single-turn bend radii. A low-loss wavelength range was observed that was bounded by loss edges at short and long wavelengths. The inset in Fig. 4 is an example of such a spectrum for the very tight bend radius of 4 mm. The variation of the short-wavelength loss edge with bend radius R is plotted in Fig. 4, together with a fit to $\lambda = \text{constant}/\sqrt{R}$. The fit is excellent, confirming the validity of relation (8) and hence of the effective index model.

The loss edge for a 5-mm bend radius was at $\sim$530 nm. The cubic dependence on Λ in relation (8) indicates that a fiber with a pitch of 10 μm and the same relative hole size would suffer bend loss at a bend radius of approximately half a meter at this wavelength. Thus bend loss limits not only the useful wavelength range of our endlessly single-mode fiber but also the otherwise appealing prospect of a single-mode fiber with a macroscopic core.

We have used an effective-index model to show that the photonic crystal fiber can, as suspected, be single mode at all wavelengths. The useful wavelength range of the fiber within the transparency window of silica, although wide, is ultimately limited by bend loss.

T. A. Birks is a Royal Society University Research Fellow. This research is supported by the UK Defence Research Agency at Malvern and the Engineering and Physical Sciences Research Council. The fiber was made by J. C. Knight at the University of Southampton.

References

1. J. C. Knight, T. A. Birks, P. St. J. Russell, and D. M. Atkin, Opt. Lett. **21,** 1547 (1996); **22,** 484 (1997).
2. A. W. Snyder and J. D. Love, *Optical Waveguide Theory* (Chapman & Hall, New York, 1983).
3. T. A. Birks, P. J. Roberts, P. St. J. Russell, D. M. Atkin, and T. J. Shepherd, Electron. Lett. **31,** 1941 (1995).
4. C. Vassallo, Opt. Quantum Electron. **15,** 349 (1983).
5. J. D. Love, Proc. Inst. Electr. Eng. Part J **13,** 225 (1989).